Tetrathiafulvalene-Based Magnets of Lanthanides

Olivier Cador, Fabrice Pointillart

1 Introduction

Magnets have been discovered about four millenniums ago in ancient Greece. Nowadays, in 2015, permanent magnets market is valued to 15 billion € and is expected to grow according to the demands for medical and industrial devices. In this market, the segment occupied by the badly named rare-earth[1]-based magnets continues to expand owing to superior properties (such as saturation magnetization).

In the 1990s, a new class of magnets emerged in the scientific community with the discovery of the single-molecule magnets (SMMs) [1]. In these magnets, the magnetic memory is stored by the magnetic moment of a single molecule constituted of 12 manganese ions. This scientific finding reduced the size of a storage unit (byte) to nanometer. At the same time, the storage capacity of hard disks based on molecules would increase drastically. The drawback is the operating temperature range, below liquid helium (−269°C). In the last three decades, the quest for better SMMs never really stopped. In 2003, Ishikawa et al. [2] discovered that a single lanthanide ion (Ln = Tb^{III}) embedded in a double-decker complex behaved as a SMM. To date, the lanthanide series is the most productive SMMs line in Mendeleev's periodic table with a recent tremendous record of closure of the magnetic hysteresis loop at 60 K [3, 4], close to liquid nitrogen.

Tetrathiafulvalene (TTF) and its analogues are well known in the field of molecular materials to produce organic metals, semiconductors, and superconductors [5, 6]. The functionalization of the electron donor TTF core by an acceptor moiety contributed to the development of functional materials such as switches, sensors, photovoltaic cells, and nonlinear optical systems [7–9]. It was then logical to adapt the acceptor moiety to coordinate transition metals for (1) elaboration of multifunctional materials with both paramagnetism and electrical conductivity [10, 11] and (2) the synthesis of polynuclear transition metal complexes exhibiting SMM properties embedded in a conducting material [12–16]. One must admit that all tentative proposals were not very successful except Oshio's work [17] which shows SMM behavior but without conductivity.

The first TTF-Ln system was reported by Faulkner et al. [18] with the assembly in solution of tetrathiafulvalene carboxylic acid and ytterbium. In 2003 [19], the first structurally characterized TTF-Ln system in the solid state was reported. There was no chemical bond between the lanthanide ion and the TTF moiety, so the chemical approach is the so-called through space. We have published almost 10 years ago the first isolated TTF-Ln coordination complex [20] based on the spin-only Gd(III) ion, which, of course, does not behave as a SMM. Since 2009, several groups [21–24], including us [25], have paid much attention to TTF-Ln systems with the objectives to combine conductivity (electrical transport), magnetism (magnetic memory), and luminescence (light emitter) in a single chemical object. In this frame, the TTF moiety turns out to be a powerful sensitizer of the NIR luminescence of

[1]Most of the rare earths are not rare: cerium is more abundant than copper on earth, and thulium (the most rare) is more abundant than silver.

lanthanides [26]. Nevertheless and despite colossal efforts of the scientific community, electrical conductivity has never been observed in TTF-Ln systems. One could say that the necessary oxidation (partial) of the TTF moiety to promote electronic transport does not preserve the chemical integrity of the complex (dissociation) except when both TTF core and coordinating moiety are not fused [27]. Despite several attempts, there is no SMM based on TTF and strongly anisotropic 3-D transition metals such as Co(II) and Ni(II) [12, 13, 28, 29]. But TTF performed in the field of SMMs with plethora of mononuclear and polynuclear complexes which possess a magnetic memory in the absence and, in less extent, in the presence of an external constant magnetic field. Since highly anisotropic magnetic moments are necessary, Dy(III) and Tb(III) are the ideal candidates [30–37]. These two ions represent almost 99% of reported Ln-based SMMs [38] with a preponderant role played by Dy(III)-based systems.

2 Preamble

Naturally, researchers have at first focused their attention on the synthesis of mononuclear TTF-Dy complexes. Like most of the time, the first attempt was not very successful [39]. The reaction of two equivalents of tetrathiafulvalene-amido-2-pyridine-*N*-oxide with $[Dy(hfac)_3]\cdot 2H_2O$ ($hfac^-$: 1,1,1,5,5,5-hexafluoroacetylacetonate anion) precursor produced mononuclear species in which Dy(III) is surrounded by eight oxygen atoms: two from pyridine-*N*-oxide moieties and six from three bidentates $hfac^-$. This fully oxygenated environment adopts a coordination polyhedron close to square antiprism (SAP) D_{4d} with CShM = 0.528 [40]. The material does not show any out-of-phase component of the AC susceptibility in zero external dc field down to 2 K below oscillating field frequencies of 1 kHz. In other words, it is not a magnet. Probably, the charge distribution around the Dy(III) center does not match the axiality required by the simple but chemically implementable precepts exposed by Rinehart et al. [41]. Performant magnets are obtained when the largest M_J states are stabilized for a given multiplet ground state ($M_J = \pm 15/2$ for Dy(III)). The analysis of the electron density distribution provides a simple tool to anticipate what might be the ground state in a given environment [42]. The charge density distribution of the Ising component (the largest M_J values) of the multiplet ground state of the oblate Dy(III) is represented on Fig. 1. The electrons are principally located in a plane (*xy*), so the disposition of negatively charged ligands in the *z* direction will stabilize this Kramers state. It is the opposite for the prolate Yb(III) for which the negative charges must lie in the *xy* plane. This textbook analysis guided the synthesis of the most efficient SMM reported so far [3, 4]. Additionally, advanced quantum calculations have demonstrated that such approach might provide high-temperature SMMs (if chemically accessible) [43, 44].

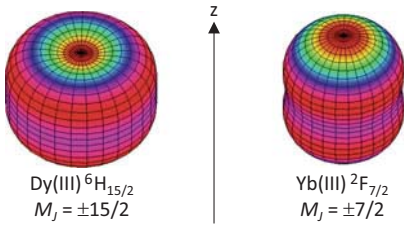

Fig. 1 Angular dependences of the total 4*f* charge density for largest M_J states of the multiplet ground state for Dy(III) and Yb(III)

3 Mononuclear TTF-Dy(III) SMMs: The N_2O_6 Saga

We have sought, at first, for neutral complexes to crystallize with bidentate TTF-based ligands in order to (1) stabilize the complexes and (2) minimize the degrees of freedom of the coordination sphere. The use of three negatively charged acetylacetonate (−1) ancillary ligands counterbalances the charge +3 of the lanthanide ions and insures complex neutrality. To complete the coordination sphere, TTF-based ligands with nitrogen-coordinating sites have been designed to desymmetrize the ligand field (preamble). The first two complexes synthesized with this approach are [Dy(hfac)$_3$**L**$^{\mathbf{1}}$] and [Dy(hfac)$_3$**L**$^{\mathbf{2}}$] (with **L**$^{\mathbf{1}}$ = 2-{4,5-[4,5-bis (propylthio)-tetrathiafulvalenyl]-1H-benzimidazol-2-yl}pyridine and **L**$^{\mathbf{2}}$ = 2-{1-methylpyridyl-4,5-[4,5-bis(propylthio)tetra-thiafulvalenyl]-1H-benzimidazol-2-yl} pyridine) [45] (Fig. 2). Except the obvious chemical difference at N3 (alkylation), the analysis of the crystallographic structure revealed the presence of intermolecular hydrogen bond at N3 site in [Dy(hfac)$_3$**L**$^{\mathbf{1}}$]. Such intermolecular connection does not exist in [Dy(hfac)$_3$**L**$^{\mathbf{2}}$], and it has a dramatic consequence on the coordination polyhedra. Indeed, the polyhedron is strongly distorted in [Dy(hfac)$_3$**L**$^{\mathbf{1}}$] with respect to the one in [Dy(hfac)$_3$**L**$^{\mathbf{2}}$] (Fig. 2). As a consequence, the magnetic properties of these two, apparently similar, complexes differ. In zero external dc field, [Dy (hfac)$_3$**L**$^{\mathbf{2}}$] behaves as a SMM with the apparition of a frequency-dependent out-of-phase component of the ac susceptibility. Such signal is absent for [Dy(hfac)$_3$**L**$^{\mathbf{1}}$] which is not a SMM, as far as the crystalline condensed phase is concerned. The hydrogen-bonding network plays a crucial role in the modification of this behavior. Magnetic measurements in solution reveal the true nature of the complexes. Of course, one must be sure that the complexes are stable in solution. They both behave the same, as molecular magnets. This proves two important characteristics: (1) the behavior of SMM can be preserved in solution. This is an important issue since one may say that the observed behavior is truly of molecular origin and then the molecular magnet can be manipulated. (2) The destruction of the intermolecular network by dissolution restores the molecular property. The absence of SMM behavior in crystalline condensed phase must be taken carefully, and the impact of the crystal packing must be analyzed prior any hasty conclusion.

The ground multiplet ground state $^6H_{15/2}$ of Dy(III) splits under the effect of crystal field in several sublevel characterized by pure M_J levels or a mixture of M_J levels depending on the symmetry of the ligand field. In this frame, the effective 1/2

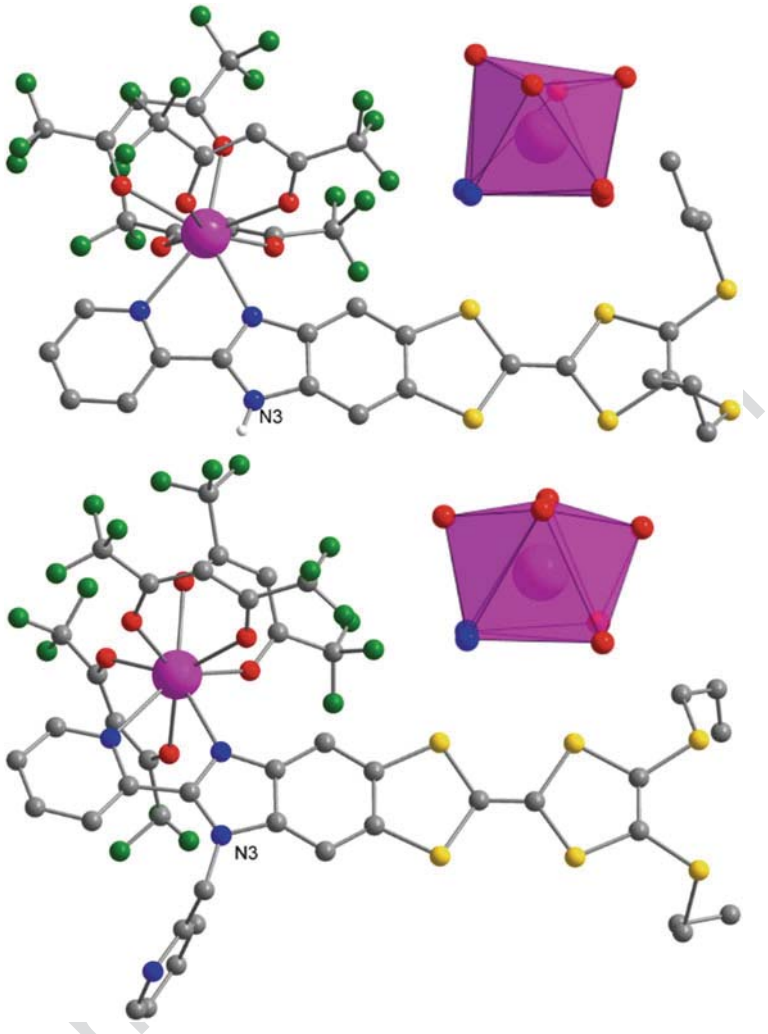

Fig. 2 Representation of the complexes [Dy(hfac)$_3$**L^1**] (top) and [Dy(hfac)$_3$**L^2**] (bottom) with the alkylated nitrogen atom N3. Coordination polyhedra are also represented

is often used to describe these Kramers sublevels. Then, the Kramers ground state possesses an effective spin 1/2 with an effective $\boldsymbol{g}$-tensor in the reference frame of the complex. It is not difficult to show that for the two Ising components $M_J = \pm 15/2$ of the $^6H_{15/2}$ multiplet the $\boldsymbol{g}$-tensor is characterized by $g_x = g_y = 0$ and $g_z = 20$ with z the axis of projection. Experimentally, the orientation and the amplitude of the $\boldsymbol{g}$-tensor are available under certain conditions: the complex must crystallize in the triclinic system with only one Dy(III) crystallographic site. Measurements of the magnetization on an oriented single crystal in three perpendicular planes as a function of the angle (θ) between the magnetic field (H) with the axes of the single

crystal allow the determination without ambiguity of the ***g***-tensor. The magnetic susceptibility in a plane can be fitted with the following equation:

$$\chi_{\mathrm{M}}T = \frac{MT}{H} = \chi_{\alpha\alpha}T\cos^2\theta + \chi_{\beta\beta}T\sin^2\theta + 2\chi_{\alpha\beta}T\sin\theta\cos\theta$$

where α and β are the directions X, Y, and Z of the crystal reference frame in a circular permutation (Fig. 3) and χ_{M} and T are, respectively, the molar magnetic susceptibility and the temperature expressed in Kelvin.

In the effective spin-1/2 frame, the principal values of ***g***-tensor are $g_z = 14.22$, $g_y = 3.96$, and $g_x = 9.43$. These values are far away from those expected for a purely axial system and explain why [Dy(hfac)$_3$**L^1**] is not a SMM in the condensed crystalline phase. The orientation of the g_z is represented on Fig. 4 with a black arrow. In the present case, in order to simulate physical properties such as magnetism, the neighboring molecules need to be explicitly integrated. The calculated orientation of the most magnetic axis is also represented on Fig. 4. Clearly, calculations with N–H bond fail to reproduce the orientation of the magnetic poles as well as the standards $\chi_{\mathrm{M}}T$ vs. T and M vs. H plots (Fig. 4 top right, M the magnetization expressed in Bohr magneton per mole) [46]. One can notice however that in this chemical configuration, the magnetic moment of a Dy(III) ion resides in a direction passing through the most negatively charged direction (two hfac$^-$ anions) and perpendicular to the plane defined with the less electronegative nitrogen atoms from imidazole and pyridine moieties, in agreement with basic electrostatic considerations. The hydrogen atom must be positioned between two heteroatoms: the nitrogen N3 of imidazole of one complex and one oxygen atom of one hfac$^-$ moiety of a neighboring complex. In other words, in the crystal, the N–H bond disappeared with a hydrogen atom, in average, localized at an intermediate position between the two atoms. Nevertheless, the calculated orientation is still at 30° of the experimental one and that dynamical effects should also probably be included to properly account for the experience.

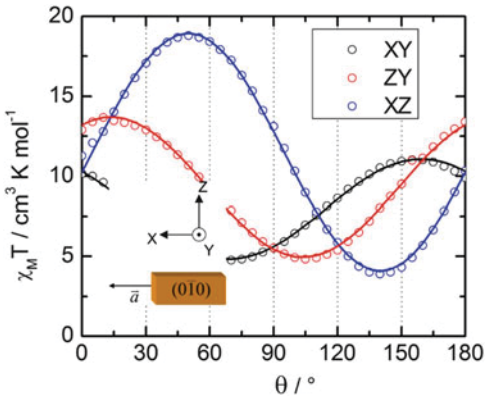

Fig. 3 Angular dependence of $\chi_{\mathrm{M}}T$ measured at 2 K for [Dy(hfac)$_3$**L^1**] with a 1 kOe magnetic field in three perpendicular planes (*XY*, *ZY*, and *XZ*). In inset a schematic representation of a single crystal of [Dy(hfac)$_3$**L^1**] with crystallographic axes in the frame of the single crystal

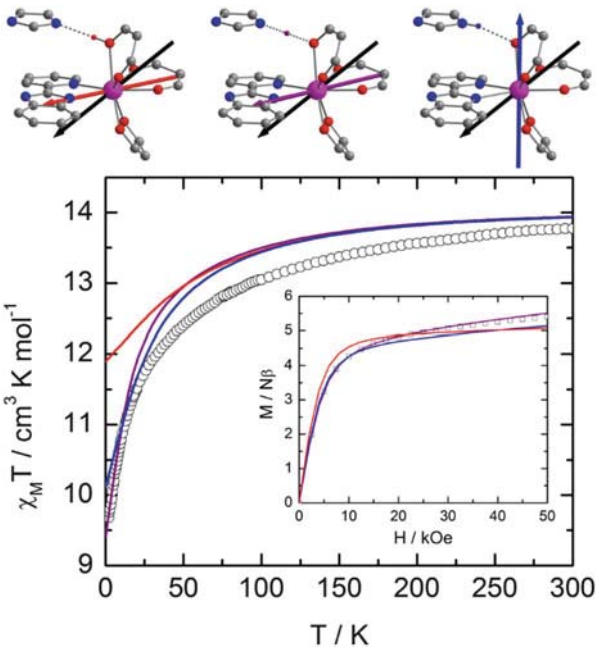

Fig. 4 (Top) orientations of the experimental z magnetic axis represented in black for [Dy(hfac)$_3$**L^1**] with the calculated orientation for different positions of the hydrogen atom (O–H in red, N–H in blue, and middle in purple). (Bottom) thermal variations of the experimental (white symbols) and calculated (full-colored lines) $\chi_M T$ within the inset of the experimental and calculated field variation of the magnetization at 2 K

At this stage **L^2** seems to be a good starting point, but the use of hfac$^-$ produces a SMM with relatively low efficiency. Indeed, the energy necessary to reverse the magnetic moment is less than 20 K (the barrier) and a temperature-independent relaxation process (quantum tunneling of the magnetization) of the order of 100 μs. In order to improve the SMM in keeping this topology, one possibility is to play with the ancillary ligand. Thiophene groups are less electroattractive than CF_3, and then the substitution of one CF_3 by one thiophene should increase the negative charges on coordinated oxygen atoms.

The magnetic properties of [Dy(tta)$_3$**L^2**] (tta$^-$: 2-thenoyltrifluoroacetonate) have been studied in the crystalline condensed phase and in frozen solution [47]. Qualitatively, the magnetism corresponds to [Dy(hfac)$_3$**L^2**]: it is a SMM in solid state and in solution. Quantitatively, the energy barrier has been multiplied by a factor two and validates our approach. Ab initio calculations showed that the negative charges carried by oxygen atoms are larger, in amplitude, than for [Dy(hfac)$_3$**L^2**] (−0.71 vs. −0.68 in average) according to electrostatic considerations [46, 47]. Interestingly, SHAPE analyses [40] on [Dy(tta)$_3$**L^2**] and [Dy(hfac)$_3$**L^2**] reveal nearly the same distortions. In both structures, Dy(III) resides in SAP environment with CShM = 0.538 and 0.597, respectively. Angular-resolved magnetometry measurements show that the anisotropy axis (the easy magnetization axis) is parallel to the most negatively charged direction (Fig. 5). This experimental finding is supported by ab initio calculations with a gap between the calculated and the experimental easy axis of only 7.6°. Furthermore, the calculated g_z (19.5) is very close to the Ising limit. The examination of the temperature dependence of the relaxation time of the

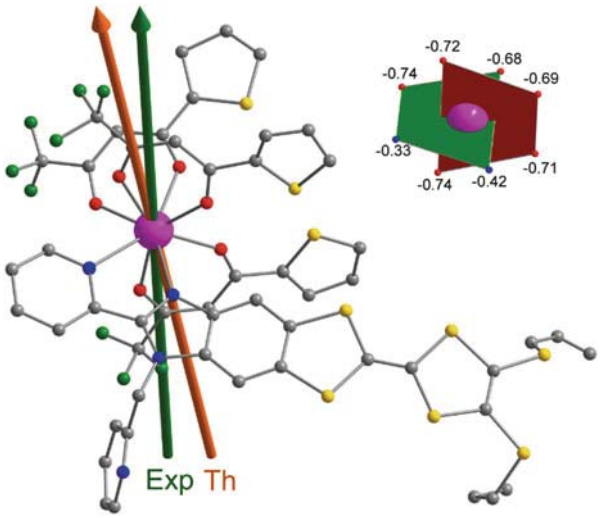

Fig. 5 Representation of the molecule $[Dy(tta)_3\mathbf{L}^2]$ avec and the calculated (orange) and experimental (green) magnetic axes. Insert: scheme of the coordination sphere of Dy (III) ion with the calculated charges of the coordinated atoms

magnetic moment reveals the presence of a thermally activated regime at a high temperature, while the system enters a thermally independent regime below 6 K (Fig. 6). It can be reproduced with a combination of the Orbach [48] (over the barrier) and tunneling (through the barrier) processes: $\tau^{-1} = \tau_0^{-1}\exp(\Delta/T) + \tau_{TI}^{-1}$ with Δ=42 K, $\tau_0 = 8 \times 10^{-6}$ s, and $\tau_{TI} = 1.62 \times 10^{-3}$ s. Dy(III) is a Kramers ion, and the magnetic moment should not be able to tunnel through the barrier: the two Ising components cannot be mixed by modulation of the crystal field. The application of a moderate external dc field (1 kOe) destroys this relaxation path, and the system falls in a pure thermally activated regime with nearly the same activation energy. Additional perturbations must affect the Kramers ground state in zero external dc field to allow the system to oscillate between the "up" and "down" states. In the condensed crystalline state, the molecules are closely packed, and interactions of dipolar origin may propagate through space. This is especially true when someone deals with heavy lanthanides which possess the largest magnetic moments of the periodic table. Transverse component of this internal field can mix the Kramers doublets and facilitate the tunneling. The dilution of the complex in a diamagnetic medium (at low concentration) minimizes this internal field and is supposed to suppress the tunneling. However, one can see on Fig. 6 that dissolution in dichloromethane is not enough: leveling of the relaxation time still persists at low temperature. Compared to the application of an external dc field of 1 kOe, which completely lifts the degeneracy of the ground state and destroys the tunneling effect (Fig. 6), in solution, the relaxation time remains rapid (about 100 times faster). The consequence is that, even in solution, the hysteresis loop remains closed in zero field while it is opened up in field (butterfly-shaped hysteresis) at any temperatures above 500 mK [47].

Then, if the closure of the hysteresis loop at the origin does not arise from intermolecular considerations, it might come from inside the complex. Dysprosium

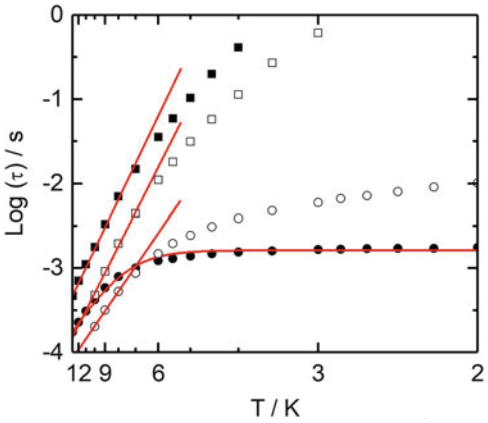

Fig. 6 Log-scale representation of the thermal variation of the relaxation time of [Dy(tta)$_3$**L^2**] in solid state (full symbols) and in solution (empty symbols), in zero external dc field (circles) and under 1 kOe external dc field (squares). Solid red lines correspond to the best fitted curves with a modified Arrhenius law at zero field and a Arrhenius law in field

is one of the elements in the periodic which consists of different and stable isotopes (^{161}Dy, ^{162}Dy, ^{163}Dy, and ^{164}Dy) in quasi-equivalent natural abundance. Two of them, with an even mass number, possess a nuclear spin ($I = 0$), and the two others have a nuclear spin $I = 5/2$. We have then decided to study the influence of this nuclear spin on the relaxation of the electronic magnetic moment [49] coupled with magnetic dilution. Hyperfine interactions and dilution are known to affect the relaxation of the magnetic moments [50–52]. Clearly, metal-centered isotopic enrichment modifies the relaxation rate in the quantum regime (Fig. 7).

Below 6 K when the system enters in the quantum regime, the relaxation time of the magnetic moment is ten times slower for the isotopically enriched complex [^{164}Dy(tta)$_3$**L^2**] ($I = 0$) than for the isotopically enriched complex [^{161}Dy(tta)$_3$**L^2**] ($I = 5/2$). This is true in zero external dc field in the condensed crystalline phase but also when the enriched complex is diluted in a diamagnetic isomorphous crystalline matrix ([^{164}Dy$_{0.04}$Y$_{0.96}$(tta)$_3$**L^2**]•C$_6$H$_{14}$ vs. [^{161}Dy$_{0.03}$Y$_{0.97}$(tta)$_3$**L^2**]•C$_6$H$_{14}$). The dramatic difference is that the dilution in a diamagnetic medium of these isotopically enriched complexes slows the relaxation enough to observe the opening of the hysteresis loop at the origin for the ^{164}Dy derivative and not for the ^{161}Dy derivative. At this stage we proved that isotopes chemistry drives some electronic properties. Nevertheless, one must keep in mind that the hysteresis (the memory) in the absence of an external stimulus shows up only when the molecules are far away from each other. Thus, the deposition of juxtaposed SMMs on surfaces can lead to unexpected results because they will behave, in a certain manner, collectively and not individually (Fig. 8).

In addition, we recently investigated the magnetism of the last two stable enriched complexes [^{162}Dy(tta)$_3$**L^2**] and [^{163}Dy(tta)$_3$**L^2**] [53]. [^{162}Dy(tta)$_3$**L^2**] is the copy paste of [^{164}Dy(tta)$_3$**L^2**] because the nuclear spin of Dy(III) is zero in both cases. The nuclear spins of ^{163}Dy and ^{161}Dy are indeed equal ($I = 5/2$), but the hyperfine coupling constant A_{HF} differs [54, 55] and then the relaxation rate affected. This is perceptible in condensed crystalline phase with [^{163}Dy(tta)$_3$**L^2**]

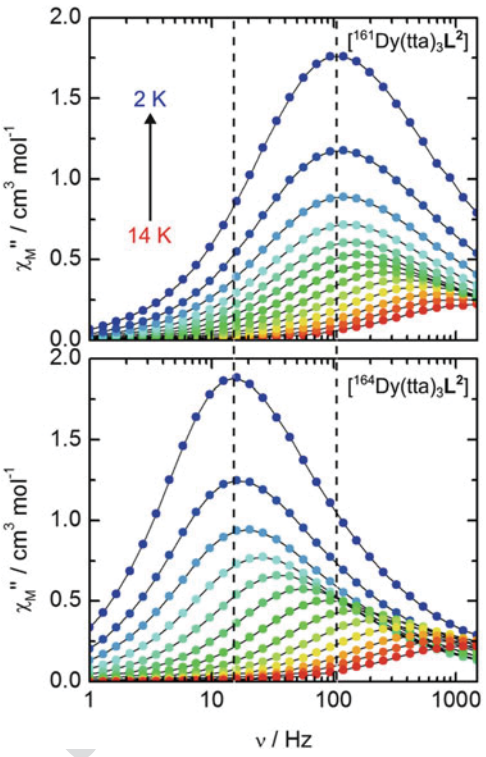

Fig. 7 Frequency dependences of χ_M'' of [^{164}Dy(tta)$_3$**L^2**] and [^{161}Dy(tta)$_3$**L^2**] in zero field in the temperature range 2–14 K

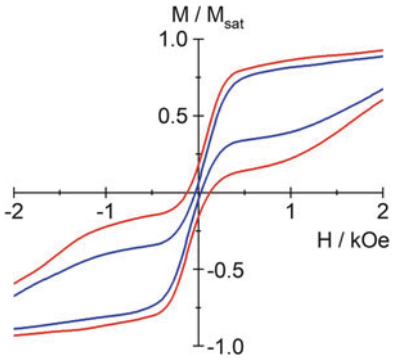

Fig. 8 Normalized magnetic hysteresis loops measured at 460 mK for [^{164}Dy$_{0.04}$Y$_{0.96}$(tta)$_3$**L^2**]•C$_6$H$_{14}$ (red line) and [^{161}Dy$_{0.03}$Y$_{0.97}$(tta)$_3$**L^2**]•C$_6$H$_{14}$ (blue line)

slightly faster than [^{161}Dy(tta)$_3$**L^2**], but at this stage, the relaxation is essentially driven by intermolecular interactions. Once diluted, [^{161}Dy$_{0.05}$Y$_{0.95}$(tta)$_3$**L^2**]•C$_6$H$_{14}$ is about ten times slower than [^{163}Dy$_{0.05}$Y$_{0.95}$(tta)$_3$**L^2**]•C$_6$H$_{14}$. Sign and/or amplitude of the hyperfine coupling seem to play also a fundamental role on the relaxation in quantum regime.

4 A Journey in TTF-Ln SMMs

There are additional TTF-Dy(III) [N_2O_6] mononuclear complexes which behave as SMMs in the literature. Also, higher coordination number, typically N_3O_6, has been envisaged with less success. Environment such as O_8 for which the charge distribution is more symmetric has also been investigated. Some of these complexes are *stricto sensu* (chemically) mononuclear complexes, but some of them are polynuclear complexes but in which the distances between metallic centers are so large that we can consider they are mononuclear from a magnetic point of view. In other words, there are no interactions between those centers. Such complexes might be described as an assembly of mononuclear SMMs.

4.1 Nitrogen-Based Donor-Acceptor Type Dyads

The first example we want to introduce is based on a similar TTF ligand with a benzothiazole group. The ligand $\mathbf{L^3}$ ($\mathbf{L^3}$ = 4-[6-(1,3-benzothiazol-2-yl)pyridin-3-yl]-4′,5′-bis(methyl-thio)tetrathiafulvene) is similar to $\mathbf{L^1}$ with however no possible intermolecular hydrogen bond [56]. Such benzothiazole group might also be of interest to realize photoswitchable conductors and photoelectric conversion materials [57]. Reaction of $\mathbf{L^3}$ with [Ln(tta)$_3$]·2H$_2$O gives [Ln(tta)$_3$$\mathbf{L^3}$] complex which crystallize in the P-1 triclinic space group for light elements and in the P2$_1$/a monoclinic space group for heavy elements. For intermediate Dy(III), the two polymorphs can be obtained. Like in the previous section, Dy(III) ion is in a N_2O_6 environment (Fig. 9) with a square antiprismatic idealized coordination polyhedron. The complexes behave as SMMs with slightly different energy barriers (57 K vs. 42 K). The coordination polyhedron is slightly more distorted in the triclinic phase than in the monoclinic one with however the highest energy barrier. One should then conclude that there is no direct correlation between symmetry and activation energy. Additional factors, which are not that clear and yet to be identified, influence the energy splitting diagram. Quantum chemistry calculations qualitatively reproduce this experimental fact: the first excited state is located higher in energy in the monoclinic phase than in the triclinic. These barriers are also similar to the one found for [Dy(tta)$_3$$\mathbf{L^2}$] (due the similarities between the two environments). Here again, the calculated and the experimental orientation of the easy magnetic axis are in very good agreement with less than 10° of mismatch and an orientation in the most negatively charged direction. The dilution+enrichment protocol has been applied to both polymorphs, but only nuclear spin-free isotopes were employed to slow down the relaxation as much as we could. The same receipts give the same results: the hysteresis loops open in zero field for the enriched and diluted complexes.

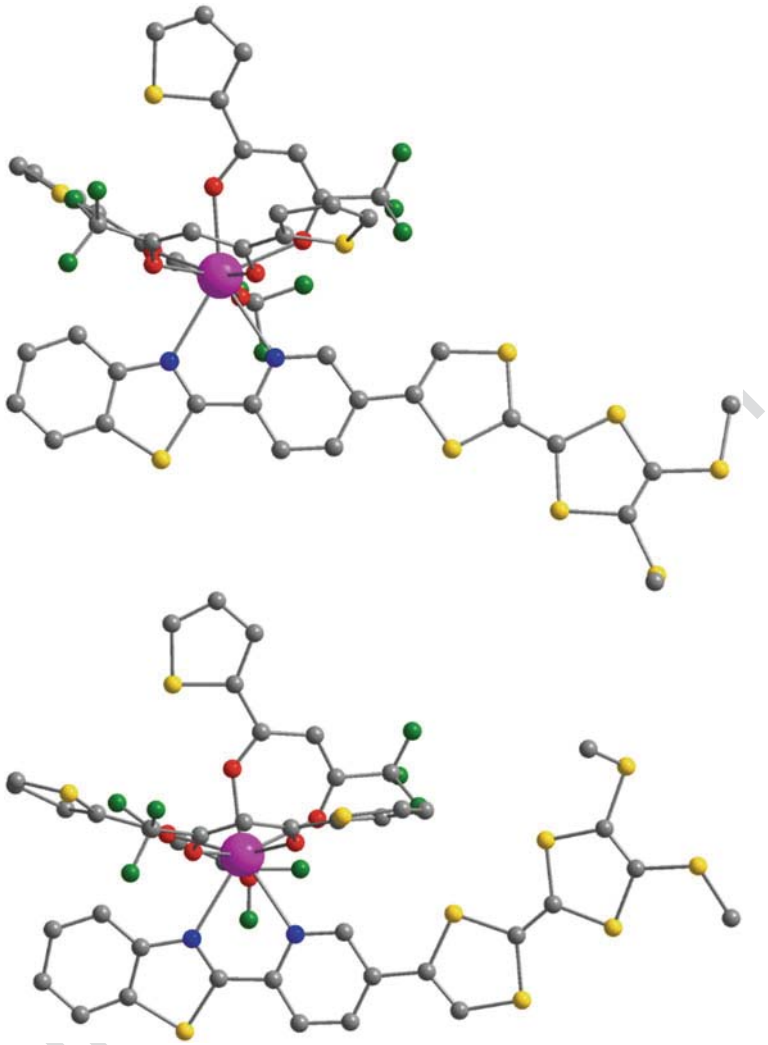

Fig. 9 Representation of the complex [Dy(tta)$_3$**L**^{3}] in the triclinic (top) and monoclinic (bottom) forms

All the TTF-based ligand envisaged so far could be coordinated only by one metal center, so we imagined and designed new TTF-based ligand to incorporate, in a bridging ligand, different coordination sites. The ideas behind were to (1) select different metals in incorporating different chelating sites (e.g., tris-) and (2) to accommodate the same metal in different environments to tune its magnetic properties (Fig. 10) [58].

When reacted with [Dy(hfac)$_3$]·2H$_2$O, **L**^{4} coordinates from both bischelating sites to form [Dy$_2$(hfac)$_6$**L**^{4}] neutral complex. Each Dy(III) ion is surrounded by six

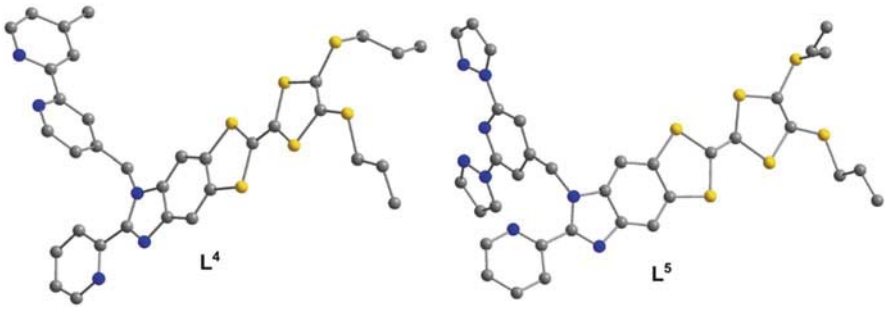

Fig. 10 Representations of $\mathbf{L^4}$ and $\mathbf{L^5}$ ligands

oxygen and two nitrogen atoms and lies in almost the same N_2O_6 D_{4d} environment and is separated by more than 10 Å [58]. From a magnetic point of view, these two sites should behave the same, and this is what is observed. Both behave as SMMs in zero external dc field, and the extended Debye analysis [59] reveals only one relaxation process. Seventy percent of the magnetic moments relax at the same frequency. The relaxation is however too fast in zero field to be quantitatively analyzed. In applying an external field to suppress the thermally independent regime, only one relaxation time that includes both sites is identified. At the optimum field, i.e., the external field for which the relaxation is the slowest (800 Oe), the thermal variation of the relaxation time does not follow the Arrhenius law expected for the Orbach process [60] but can be easily reproduced with a Raman process ($\tau = CT^n$, $C = 4.8 \times 10^{-3}$, and $n = 6.26$). This tends to prove that the relaxation does not occur through the first excited state, at least, as long as the in-field relaxation is concerned.

The reaction of $[Dy(hfac)_3]\cdot 2H_2O$ with $\mathbf{L^5}$ leads to dinuclear species ($[Dy_2(hfac)_6\mathbf{L^5}]$) with two different coordination polyhedra [61], N_2O_6 ($CShM_{SAPR\text{-}8}$ (D_{4d}) = 0.435) and N_3O_6 ($CShM_{TCTPR\text{-}9}$ (D_{3h}) = 0.586). The N_2O_6 sites behave in a standard way (SMM in zero external field), while the nonacoordinated site does not show any out-of-phase signal in zero external field. The application of a moderate external dc field slows down the relaxation with the emergence of two identifiable processes that can be safely attributed to the two different sites. An extended Debye model featuring two relaxation times has been employed to treat the ac data. Interestingly, the analyses reveal the ratio of the magnetic susceptibility which relaxes at the two relaxation time to be close to 50:50 in agreement with the chemical structure. Furthermore, the energy barrier for the octacoordinated site is in good agreement with its mononuclear equivalent [45]. From a chemical point of view, it was interesting to look for site selectivity with regard to different Dy(β-diketonate)$_3$ precursors. A 1:1 ratio of $[Dy(hfac)_3]\cdot 2H_2O$ and $[Dy(tta)_3]\cdot 2H_2O$ was reacted with $\mathbf{L^5}$, and it forms dinuclear species

$[Dy_2(hfac)_3(tta)_3\mathbf{L^5}]$. The crystal structure of the complex reveals ligand exchange, with the N_2O_6 site made of two tta^- and one $hfac^-$ ligands and the N_3O_6 site made of one tta^- and two $hfac^-$ ligands. We think this ligand exchange occurs as a consequence of a subtle balance between the size of the metallic precursors and the coordination which leads to a minimum steric hindrance. The magnetic behaviors of these two metallic sites are qualitatively identical to $[Dy_2(hfac)_6\mathbf{L^5}]$ with the N_2O_6 site being a SMM in zero field while the N_3O_6 site being a SMM only in field [61].

At this stage, it appears that N_2O_6 coordination polyhedron around Dy(III) systematically produces SMMs in zero field. Liu et al. [62] developed a TTF-fused donor-acceptor system based on dipyrido[3,2-*a*:2′,3′-*c*]phenazine (dppz) which can be reacted with Dy(β-diketonate)$_3$ precursors ($[Dy(hfac)_3]\cdot 2H_2O$ and $[Dy(tta)_3]\cdot 2H_2O$) [63]. Two mononuclear units are obtained with Dy(III) in the standard N_2O_6 SAP coordination polyhedron made of three β-diketonate ligands and one dipyridyl moiety ($CShM_{SAPR\text{-}8}$ (D_{4d}) = 0.724 for the $hfac^-$ derivative and $CShM_{SAPR\text{-}8}$ (D_{4d}) = 0.507 for the tta^- derivative) from the ligand $\mathbf{L^6}$ ($\mathbf{L^6}$ = TTF-fused dipyrido[3,2-*a*:2′,3′-*c*]phenazine). Both compounds behave as SMM in zero field, but they are "faster," and they relax at higher frequencies, than previous N_2O_6 systems with however the tta^- derivative slower than the $hfac^-$. Typically, at 2 K, the maximum on the χ_M'' vs. ν curves shows up at 700 Hz for $[Dy(tta)_3\mathbf{L^6}]$, while it is located above 1,500 Hz for $[Dy(hfac)_3\mathbf{L^6}]$. To compare, for $[Dy(hfac)_3\mathbf{L^2}]$, the maximum was at 970 Hz and at 56 Hz for $[Dy(tta)_3\mathbf{L^2}]$ in the same sample environment. Such comparison, if natural, is however dangerous since in the low-temperature regime, where thermally independent processes take over all the others, the relaxation in the condensed crystalline phase is governed by the combination of magnetic intermolecular interactions (of dipolar origin) and hyperfine coupling. One can say that this N_2O_6 topology (three bischelating oxygenate ligand and one bischelating nitrogenated ligand) provides efficient magnets that qualitatively behave the same and quantitatively almost the same. The difference resides in the electron withdrawing or donating ability of the chemical groups on the β-diketonate ligands.

5 Oxygen-Based TTF-Based Ligands

The strong oxophilic characters of lanthanide authorize the synthesis of fully oxygenated coordination polyhedron around metal centers. However, such environment does not, a priori, create the expected dissymmetry of charges to produce SMMs in the specific case of Dy(III) at least as far as O_8 environments are concerned. The reaction of $[Dy(hfac)_3]\cdot 2H_2O$ with 4,4′,7,7′-tetra-*tert*-butyl-2,2′-bi-1,3-benzodithiole-5,5′,6,6′-tetrone ligand [64] ($\mathbf{L^7}$) forms a dinuclear complex $[Dy_2(hfac)_6(H_2O)_2\mathbf{L^7}]$ [65]. In this complex, two Dy(III) ions, related by an inversion center, in O_9 coordination polyhedron, are linked by an acceptor-donor-acceptor triad (Fig. 11). Eight of the nine are coming from bischelating ligands (three $hfac^-$ and one quinone), and the last one is coming from a water molecule. The intramolecular

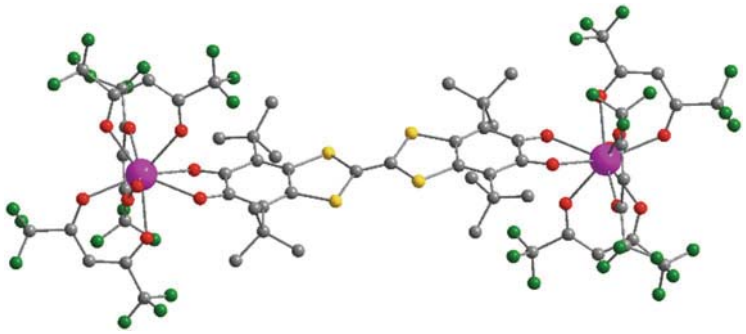

Fig. 11 View of the dinuclear compound $[Dy_2(hfac)_6(H_2O)_2\mathbf{L^7}]$

Dy-Dy distance is close to 17.5 Å, so there is no superexchange interaction between the two metals.

In this environment, Dy behaves as a SMM in zero external field. Interestingly, the equivalent complex obtained from the reaction of $\mathbf{L^7}$ with $[Dy(tta)_3]\cdot 2H_2O$ does not produce SMM. The steric hindrance of tta^- avoids water molecule to coordinate Dy(III), and therefore in this dinuclear complex, the coordination polyhedron is only made of eight oxygen atoms which is probably less suitable to promote axial anisotropy. This simple analysis is counterbalanced by other investigations [66] which clearly demonstrate that O_8 environment could perfectly produce SMMs with Dy(III) ions. Probably, the primary approach which consists of considering only the point charge model might be oversimplified. Some authors pointed out with a deeper analysis that dipole and quadrupole moments in the electrostatic potential expansion play a significant role on the magnetic anisotropy [67, 68].

To conclude this section, we would like to briefly discuss one peculiar system. Two different TTF-based ligands are used to produce a dinuclear Yb (III)-based complex $[Yb(tta)_2\mathbf{L^8}\mathbf{L^9}]_2$ [69]. The redox active ligand 4,5-bis (thiomethyl)-4′-carboxylictetrathiafulvalene ($\mathbf{L^8}$) is bridging two Yb(III) ions through $\mu_2(\eta_1,\eta_2)$ oxygen atoms, and 4,5-bis(thiomethyl)-4′-ortho-pyridyl-N-oxide-carbamoyl-tetrathiafulvalene ($\mathbf{L^9}$) is terminal (Fig. 12). The coordination sphere around each Yb(III) is made of eight oxygen atoms, and the two ions are separated by only 3.89 Å.

The static magnetic properties reveal what could be analyzed as a sign of ferromagnetic interactions between the two $^2F_{7/2}$ multiplet ground states. Indeed, on cooling from room temperature, $\chi_M T$ decreases continuously in agreement with the thermal depopulation of M_J states, passes through a broad minimum at 9 K, and then slightly increases on cooling further down to the lowest temperature. We have attempted to fit the $\chi_M T$ vs. T plot taking into account the crystal field effects by the extended Stevens operators technique [48] and the interaction between magnetic moments. The Hamiltonian to consider is the following:

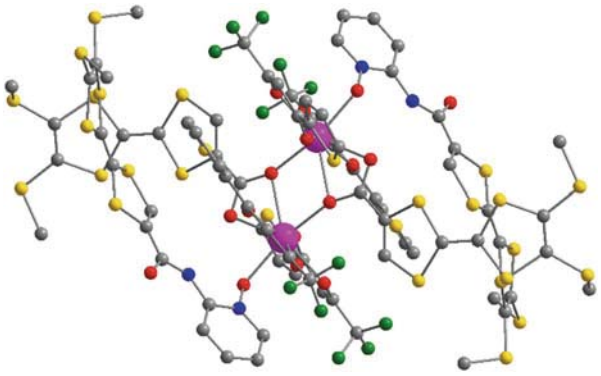

Fig. 12 View of the dinuclear compound [Yb(tta)$_2$**L**$^{\mathbf{8}}$**L**$^{\mathbf{9}}$]$_2$

$$\widehat{H}=\sum_{i=1}^{2}\left(B_2^0\widehat{\boldsymbol{O_2^0}\boldsymbol{i}}+B_2^2\widehat{\boldsymbol{O_2^2}\boldsymbol{i}}+B_4^0\widehat{\boldsymbol{O_4^0}\boldsymbol{i}}+B_4^2\widehat{\boldsymbol{O_4^2}\boldsymbol{i}}+B_4^4\widehat{\boldsymbol{O_4^4}\boldsymbol{i}}+B_6^0\widehat{\boldsymbol{O_6^0}\boldsymbol{i}}+B_6^2\widehat{\boldsymbol{O_6^2}\boldsymbol{i}}+B_6^4\widehat{\boldsymbol{O_6^4}\boldsymbol{i}}+B_6^6\widehat{\boldsymbol{O_6^2}\boldsymbol{i}}\right)$$
$$+\beta\left(g_J\widehat{\boldsymbol{J_1}}+g_J\widehat{\boldsymbol{J_2}}\right)\cdot\vec{H}-J\widehat{\boldsymbol{J_1}}\cdot\widehat{\boldsymbol{J_2}} \quad (1)$$

The first line corresponds to the crystal field effect at the two lanthanide sites with $\widehat{\boldsymbol{O_k^q}}$ the operator equivalents which can be expressed as polynomials of the total angular momentum matrices ($\boldsymbol{J^2}$, $\boldsymbol{J_z}$, $\boldsymbol{J_+}$, and $\boldsymbol{J_-}$) associated with the $^2F_{7/2}$ multiplet ground state. The second line corresponds to the Zeeman effects on $\boldsymbol{J_i}$ which are coupled through J. A homemade program has been developed to fit the magnetic data. Surprisingly a fairly good agreement (Fig. 13) is obtained without any interaction ($J = 0$ cm^{-1}), so one can consider this dimer as two isolated Yb(III) centers. The wave function analysis reveals that the Kramers ground state is the pure $M_J = \pm 7/2$ component, separated only by 2.6 cm^{-1} from the first excited state $M_J = \pm 1/2$. The stabilization of the largest M_J component can be viewed in the frame of point charge model. The carboxylate group acts as a tweezer which projects the -1 charge in a plane containing two hfac$^-$ ligands (Fig. 12). Then, ligand charges are condensed in a plane around this prolate ion (Fig. 1) and stabilize the largest M_J doublet state.

As a consequence of this Ising-type anisotropy, the complex behaves as a SMM with however a small energy barrier (~21 K) determined from the temperature dependence of the relaxation time. This value can be compared with estimated gap between the ground and the first excited states (see above, ~4 K) from DC magnetic measurements. To support this interpretation, luminescence provides a unique tool to probe energy levels. The low-temperature (77 K) excitation of the sample at 20,000 cm^{-1} sensitizes the $^2F_{5/2} \rightarrow {}^2F_{7/2}$ transitions in the range of 10,400–9,400 cm^{-1}. The excitation corresponds to LLCT (ligand-to-ligand charge transfer) and highlights the role of antenna played by the redox-active TTF ligands. We must mention that Dy(III) luminescence cannot be probed with TTF-based ligand since the emission lines fall in the absorption bands of the ligands. The

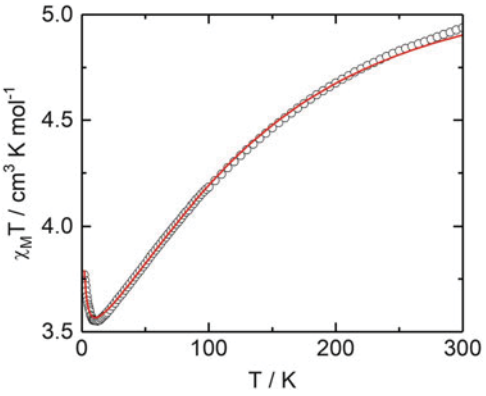

Fig. 13 Temperature dependences of $\chi_M T$ (open circles) with the best fitted curve (red line)

emission profile can be deconvoluted in four transitions (9,703, 9,936, 10,197, and 10,213 cm^{-1}). The gap between the two most energetic transitions (23 K) gives the exact gap between the Kramers doublet ground state and the first excited state. It is almost in perfect agreement with magnetism.

6 Polynuclear TTF-Dy(III) SMMs

One question emerges from the previous paragraph. Does the nonexistence of interactions between Yb(III) in Yb derivative $[Yb(tta)_2\mathbf{L^8L^9}]_2$ can be generalized to other lanthanide? The synthesis of $[Dy(tta)_2\mathbf{L^8L^9}]_2$, isostructural of Yb derivative, provides an answer [70]. On cooling, $\chi_M T$ vs. T plot passes through a broad minimum at 16 K that cannot be reproduced without taking into account interactions. The best fits are obtained with a ferromagnetic interaction $J = 2.98 \times 10^{-3}$ cm^{-1}. This interaction is very weak with respect to the energy engaged in crystal field splitting (hundreds of wave numbers). In this frame the Kramers ground state for each Dy(III) ion corresponds to more than 99% of the $M_J = \pm 15/2$. In this effective spin-1/2 model, one expects $g = 20$ in one direction and 0 in a perpendicular plane. Then, the coupling of dipolar origin between the two magnetic moment can be easily calculated from the Hamiltonian $\widehat{H} = -J_{dd}\widehat{\boldsymbol{\sigma_1}} \cdot \widehat{\boldsymbol{\sigma_2}}$ where $\widehat{\boldsymbol{\sigma}_i}$ are the operators associated with the effective 1/2 and $J_{dd} = -(\mu_0 g^2 \beta^2 / 4\pi hcr^3)(1 - 3\cos^2\theta)$ cm^{-1} (r is the distance between the metal centers, and θ is the angle between the anisotropy axis and the r vector). Such interaction can be ferro- or antiferromagnetic depending on θ. The amplitude can also be rather large at short distances, with $r = 4$ Å J_{dd} varies from –2 to +5 cm^{-1}, to compare with $J = 0.67$ cm^{-1} estimated from DC measurements in the same spin-1/2 model ($2.98 \times 10^{-3} \times 15 \times 15$). Transferred to Yb(III) system, the interaction of dipolar origin is more than six times stronger in the very hypothetical case of identical θ. Taking into account the interaction between the two Ising centers, we can describe the ground state with two components: $|\uparrow\uparrow\rangle$ and

$|\downarrow\downarrow\rangle$ separated by $J/2$ (0.335 cm^{-1}) from the excited state described by $|\uparrow\downarrow\rangle$ and $|\downarrow\uparrow\rangle$. The complex is a SMM. However, the thermal variation of the relaxation time at low temperature is very different from what we are used to observe on mononuclear complexes. Indeed, there is no leveling of the relaxation time on cooling in zero external dc field down to 2 K: τ increases continuously on cooling. This is certainly the consequence of the thermal population of the four levels. Remarkably, within an external DC field, τ does not greatly vary. This is a consequence of the condensation of the four states on few tenths of wave numbers.

The implication of magnetic interactions on slow relaxation dynamics in dimers is confirmed by other investigations on TTF-based Dy(III) dinuclear complexes. The reaction of tetrathiafulvalene-3-pyridine-N-oxide ligand ($\mathbf{L^{10}}$) with $[Dy(tta)_3]\cdot 2H_2O$ gives the centrosymmetric complex $[Dy(tta)_3\mathbf{L^{10}}]_2$ [39]. The $\chi_M T$ vs. T plot shows strong antiferromagnetic interactions between $^6H_{15/2}$ multiplets. In the effective spin-1/2 model, the interaction is estimated at -2.3 cm^{-1} with a g value (19.2) close to the Ising limit (20). The nonmagnetic ground state is then described by $|\uparrow\downarrow\rangle$ and $|\downarrow\uparrow\rangle$, with the first excited state ($|\uparrow\uparrow\rangle$ and $|\downarrow\downarrow\rangle$) at 1.3 cm^{-1}. Despite the nonmagnetic nature of the ground state, $[Dy(tta)_3\mathbf{L^{10}}]_2$ behaves as a SMM (Fig. 14). The thermal variation of the relaxation time τ does not follow a simple mathematical law since various energy levels are involved at temperatures as low as 2 K. The application of an external dc field corroborates the interpretations based on dc measurements. The field behavior of τ does reflect the low-level energy diagram.

At low field and temperatures below 8 K, τ decreases with the field (Fig. 15) with a clear dip at 1.6 kOe. At such temperatures, the first magnetically active ($|\uparrow\uparrow\rangle$ and $|\downarrow\downarrow\rangle$) excited states are thermally populated. It must be pointed out that the transition between these two states necessitates to flip simultaneously both magnetic moments, so the transition probability is very small and the relaxation time long. On increasing the magnetic field, there is a crossing between levels (Fig. 15), and, at the intersection, transition between two states involves "only" to flip one magnetic moment, and the relaxation time shortens. The minimum of τ should occur at a field which can be related to the interaction between Dy(III). With $J = -2.3$ cm^{-1}, the crossing should occur at 1.3 kOe which relatively close to the measured value. This in-field behavior

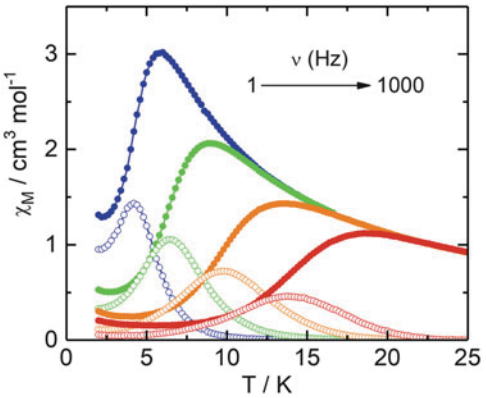

Fig. 14 Temperature dependences of χ_M' and χ_M'' measured at 1 Hz (black), 10 Hz (light gray), 100 Hz (mid gray), and 1,000 Hz (dark gray) for $[Dy(tta)_3\mathbf{L^{10}}]_2$ in the absence of an external dc field. Full symbols correspond to χ_M' and empty symbols to χ_M''

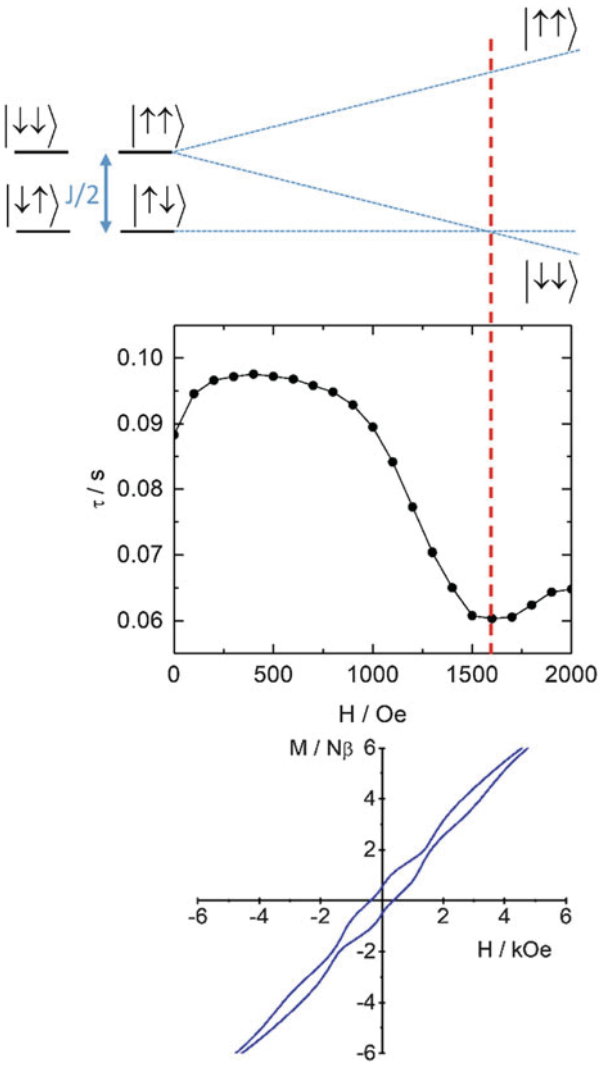

Fig. 15 (Top) field dependence of the relaxation time τ at 5 K with the magnetic field evolution of the energy levels in an Ising pattern for $[Dy(tta)_3\mathbf{L^{10}}]_2$. (Bottom) hysteresis loop for $[Dy(tta)_3\mathbf{L^{10}}]_2$ measured at 1.5 K at a sweep rate of 66 Oe s^{-1}

has also a consequence on the magnetic hysteresis. At 1.5 K, the magnetic hysteresis loop measured at 66 Oe s^{-1} differs significantly from those of mononuclear species (Fig. 15) [71]. The butterfly transforms into a double butterfly. The neck at 1.3 kOe traduces the acceleration of the relaxation at crossing field. In addition, the loop is opened at the origin. One may say that this nonmagnetic object possesses a magnetic memory anyway.

$[Dy(hfac)_2(SO_3CF_3)\mathbf{L^{11\bullet+}}]_2$ is another example of dinuclear TTF-Ln-based complexes [27] with 4,5-bis(3-pyridyl-N-oxidemethylthio)-4′,5′-methyldithiotetrathiafulvene ligand ($\mathbf{L^{11}}$). This complex has some common points with $[Dy(tta)_3\mathbf{L^{10}}]_2$: the coordination polyhedron is made of eight oxygen atoms, and

pyridine *N*-oxide bridges two Dy(III) ions. However, in this system, one monoanionic β-diketonate moiety has been substituted by one monoanionic sulfonate. One oxygen atom from pyridine *N*-oxide group completes the coordination sphere. The ligand $\mathbf{L^{11}}$ has been oxidized during galvanostatic. The TTF core is almost planar in agreement with its radical cationic form $\mathbf{L^{11\bullet+}}$. Two non-coordinated sulfonate anions balance the positive charge of the complex. In the crystal lattice, the TTF cores are dimerized with short intermolecular S···S contacts (~3.35 Å), and then the radicals are magnetically inactive (strongly antiferromagnetically coupled). This is confirmed by the very weak EPR signal centered at g~2.007 measured at 77 K. The electrical resistivity measured at room temperature on single crystals corresponds to an insulator. The analysis of the static magnetic properties reveals a weak antiferromagnetic coupling ($J = -3 \times 10^{-3}$ cm^{-1} according to Eq. 1) and a Kramers ground state mainly constituted of $M_J = \pm 13/2$. The χ_M'' vs. ν curves at zero field does not pass through the characteristic maximum at low temperature, so even if it is clear that $[Dy(hfac)_2(SO_3CF_3)\mathbf{L^{11\bullet+}}]_2$ behaves as a SMM, it is less efficient than the previous example probably because the environment around the lanthanide is chemically different.

The last two examples we would like to tackle are polynuclear complexes which feature more than two metal centers. The rational design of a lanthanide-based complex featuring different lanthanide motifs can be safely envisaged in combining $[Dy(tta)_3\mathbf{L^{10}}]_2$ and $[Dy(tta)_3\mathbf{L^2}]$. To do so a TTF-based ligand has been designed to feature a bridging site of pyridine *N*-oxide type and a bischelating nitrogen-based site [72]. The ligand 2-{1-methylpyridine-N-oxide-4,5-[4,5-bis(pro-pylthio)tetrathiafulvalenyl]-1H-benzimidazol-2-yl}pyridine ($\mathbf{L^{12}}$) was then treated with two equivalents of $[Dy(tta)_3]\cdot 2H_2O$ to give the complex $[Dy_4(tta)_{12}(\mathbf{L^{12}})_2]$ (Fig. 16). In the complex, the reader will recognize one moiety similar to $[Dy(tta)_3\mathbf{L^{10}}]_2$ and two moieties similar to $[Dy(tta)_3\mathbf{L^2}]$. The distance between these moieties (metal-metal) is above 10 Å, so there is no direct interaction between these three distinct SMMs. The magnetism of this object should coincide with the superposition of two different SMMs.

In zero external field, the χ_M'' vs. ν curves at various temperatures between 2 and 11 K clearly show two well-separated relaxations which can be confronted to the measurements on the isolated species. The presence of a slow and a fast process at low and high frequencies, respectively, matches almost perfectly with the isolated species. The low-frequency side corresponds to the dinuclear part and the high frequency to the mononuclear. It is also possible to analyze quantitatively the thermal and the in-field behaviors with a combination of two extended Debye models. At this stage our synthetic approach allowed us to conceive a complex which contains two different SMMs which act differently in the temperature and time scales. This rational design is very promising to elaborate multifunctional complexes (Fig. 17).

The last example we would like to comment concerns the polymeric species. $[Yb(hfac)_3]\cdot 2H_2O$ was reacted with the disodium salt of $\mathbf{L^{13}}$ with $\mathbf{H_2L^{13}}$ = 4,5-bis(carboxylic)-4′,5′-methyldithiotetrathiafulvene in dimethylformamide (DMF) to produce $\{[Yb\mathbf{L^{13}}(H_2O)_3(DMF)]\cdot(\mathbf{HL^{13}})\cdot(H_2O)\}_n$ [73]. The monodimensional

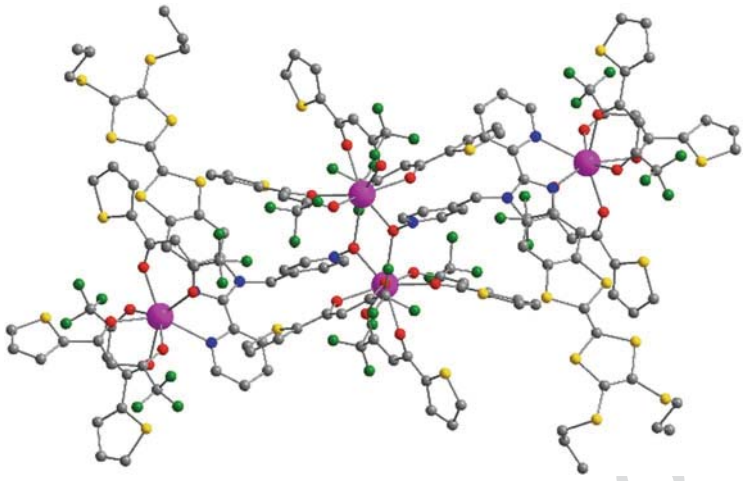

Fig. 16 Single-crystal X-ray structure of the tetranuclear complex $[Dy_4(tta)_{12}(\mathbf{L^{12}})_2]$

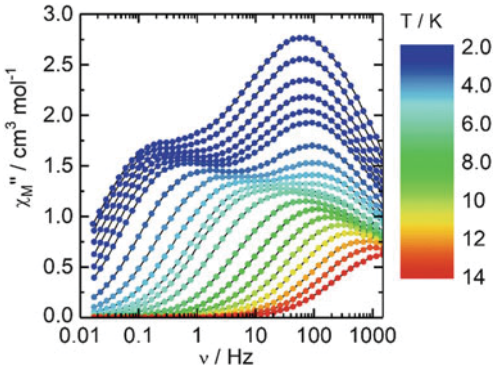

Fig. 17 Temperature and frequency dependence of the out-of-phase component of the ac susceptibility $[Dy_4(tta)_{12}\mathbf{L^{12}}_2]$ measured in zero external dc field

polymer consists of chain of Yb(III) bridged by carboxylate anions in a $\mu_2(\eta_1,\eta_1)$ mode (Fig. 18). Coordination compounds of lanthanide ions with TTF-based ligands are not so common and are essentially 0D. This is the first example of coordination polymer of lanthanide with TTF-based ligand. The coordination polyhedron is made of eight oxygen atoms in a D_{4d} environment ($CShM_{SAPR\text{-}8} = 0.454$). Our efforts to produce the dysprosium derivative were unsuccessful. It must be mentioned that no $hfac^-$ anions are present in the structure and that the polymer cannot be obtained from nitrate or halogenate salts of Yb(III). The system crystallizes in the triclinic space group $P\bar{1}$ with one Yb(III) site, so the g-tensor can be extracted from single-crystal rotating magnetometry. In the effective spin-1/25 model, $g_x = 3.24$, $g_y = 1.53$, and $g_z = 4.25$. These values are far away from the Ising limit for which

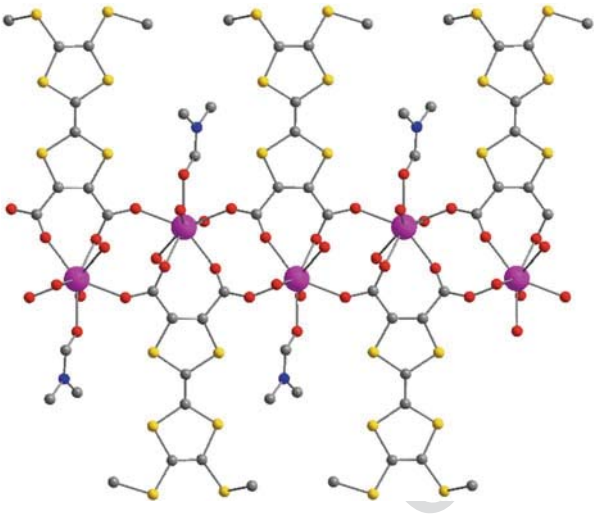

Fig. 18 Representation of the one-dimensional structure. The counterion $(\mathbf{HL^{13}})^-$ has not been represented

$g_x = g_y = 0$ and $g_z = 8.00$. As a result, the polymer does not behave as a SMM in zero external dc field. Only when an external dc field is applied that χ_M'' shows up. g_z orientation almost coincides with the fourfold axis of the square antiprism. We tentatively tried to reproduce the static magnetic properties using the ab initio CASSCF/PT2/SI-SO approach. Unfortunately, all tentative efforts failed to properly reproduce the magnetic susceptibility and magnetization curves. This underlines the difficulties already observed in the literature to efficiently model both the wave function and the energy of the low-lying multiplets of Yb(III) complexes.

7 Conclusions

In this chapter we wish to have convinced the reader that TTF-based ligands can be employed to produce SMMs. We have focused the first part of this chapter on strategies to enhance the magnetic performance of Dy-based SMM in a N_2O_6 environment. A simple molecular engineering consisting in the modulation of the electron withdrawing strength of the β-diketonate ancillary ligand highlighted the importance of the electron charge density carried by the first neighboring atom to control the energy crystal splitting and well isolate the ground multiplet state. The canceling of the intermolecular (hydrogen bond and dipolar) interactions, thanks to magnetic dilutions and spin-free isotopic enrichment, showed their efficiency to decrease the quantum tunneling of the magnetization and therefore optimize the magnetic properties of the SMM. Then the influence of the nature of the coordination sphere was studied by the analysis of mononuclear SMM library in which the Dy(III) is in N_2O_6, N_3O_6, O_8, and O_9 environments. When the Dy(III) is placed in a N_2O_6 environment, the Ising character of the magnetic anisotropy is enhanced compared to

the N_3O_6 environment. In a general manner, SMM behavior is detected when the negative charge is localized along an axis and in a plan, respectively, for the Dy(III) and Yb(III) ions [41]. In a second part, we have increased the nuclearity of the complexes. The role of the intramolecular magnetic interactions on the slow magnetic relaxation has been demonstrated.

Finally it is worth to notice that a large panel of theoretical and experimental tools is available and can be used to reach a high level of understanding of the lanthanide SMM magnetic properties, i.e., experimental measurements of the angular dependence of the magnetization, correlation between magnetism and experimental luminescence, crystal-field determination by Stevens method, and ab initio calculations.

References

1. Sessoli R, Gatteschi D, Caneschi A, Novak MA (1993) Magnetic bistability in a metal-ion cluster. Nature 365:141–143
2. Ishikawa N, Sugita M, Ishikawa T, Koshihara S, Kaizu Y (2003) Lanthanide double-decker complexes functioning as magnets at the single-molecular level. J Am Chem Soc 125:8694–8695
3. Guo F-S, Day BM, Chen Y-C, Tong M-L, Mansikkamäki A, Layfield RA (2017) A dysprosium metallocene single-molecule magnet functioning at the axial limit. Angew Chem Int Ed 56:11445–11449
4. Goodwin CAP, Ortu F, Reta D, Chilton NF, Mills DP (2017) Molecular magnetic hysteresis at 60 kelvin in dysprosocenium. Nature 548:439–442
5. Kobayashi H, Kobayashi A, Cassoux P (2000) BETS as a source of molecular magnetic superconductors (BETS = bis(ethylenedithio)tetraselenafulvalene). Chem Soc Rev 29:325–333
6. Coronado E, Galán-Mascarós JR, Gómez-García CJ, Laukhin V (2000) Coexistence of ferromagnetism and metallic conductivity in a molecule-based layered compound. Nature 408:447–449
7. Yamada J, Sugimoto T (2004) TTF chemistry: fundamentals and applications of tetrathiafulvalene. Kodansha, Tokyo, Springer, Berlin
8. Bendikov M, Wudl F, Perepichka DF (2004) Tetrathiafulvalenes, oligoacenenes, and their buckminsterfullerene derivatives: the brick and mortar of organic electronics. Chem Rev 104:4891–4946
9. Gorgues A, Hudhomme P, Sallé M (2004) Highly functionalized tetrathiafulvalenes: riding along the synthetic trail from electrophilic alkynes. Chem Rev 104:5151–5184
10. Lorcy D, Bellec N, Fourmigué M, Avarvari N (2009) Tetrathiafulvalene-based group XV ligands: Synthesis, coordination chemistry and radical cation salts. Coord Chem Rev 253:1398–1438
11. Pointillart F, Golhen S, Cador O, Ouahab L (2013) Paramagnetic 3d coordination complexes involving redox-active tetrathiafulvalene derivatives: an efficient approach to elaborate multiproperties materials. Dalton Trans 42:1949–1960
12. Gavrilenko KS, Gal YL, Cador O, Golhen S, Ouahab L (2007) First trinuclear paramagnetic transition metal complexes with redox active ligands derived from TTF: $Co_2M(PhCOO)_6(TTF\text{-}CHCH\text{-}py)_2{\cdot}2CH_3CN$, $M = Co^{II}, Mn^{II}$. Chem Commun 280–282
13. Benbellat N, Gavrilenko KS, Le Gal Y, Cador O, Golhen S, Gouasmia A, Fabre J-M, Ouahab L (2006) Co(II)−Co(II) paddlewheel complex with a redox-active ligand derived from TTF. Inorg Chem 45:10440–10442

14. Kolotilov SV, Cador O, Pointillart F, Golhen S, Le Gal Y, Gavrilenko KS, Ouahab L (2010) A new approach towards ferromagnetic conducting materials based on TTF-containing polynuclear complexes. J Mater Chem 20:9505–9514
15. Liu S-X, Ambrus C, Dolder S, Neels A, Decurtins S (2006) A dinuclear Ni(II) complex with two types of intramolecular magnetic couplings: Ni(II)−Ni(II) and Ni(II)−TTF•+. Inorg Chem 45:9622–9624
16. Cui L, Geng Y-F, Leong CF, Ma Q, D'Alessandro DM, Deng K, Zeng Q-D, Zuo J-L (2016) Synthesis, properties and surface self-assembly of a pentanuclear cluster based on the new π-conjugated TTF-triazole ligand. Sci Rep 6:srep25544
17. Mitsumoto K, Nishikawa H, Newton GN, Oshio H (2012) Encapsulation controlled single molecule magnetism in tetrathiafulvalene-capped cyanide-bridged cubes. Dalton Trans 41:13601–13608
18. Faulkner S, Burton-Pye BP, Khan T, Martin LR, Wray SD, Skabara PJ (2002) Interaction between tetrathiafulvalene carboxylic acid and ytterbium DO3A: solution state self-assembly of a ternary complex which is luminescent in the near IR. Chem Commun 1668–1669
19. Cui H, Otsuka T, Kobayashi A, Takeda N, Ishikawa M, Misaki Y, Kobayashi H (2003) Structural, electrical, and magnetic properties of a series of molecular conductors based on BDT-TTP and lanthanoid nitrate complex anions (BDT-TTP = 2,5-bis(1,3-dithiol-2-ylidene)-1,3,4,6-tetrathiapentalene). Inorg Chem 42:6114–6122
20. Pointillart F, Le Gal Y, Golhen S, Cador O, Ouahab L (2009) 4f Gadolinium(III) complex involving tetrathiafulvalene-amido-2-pyrimidine-1-oxide as a ligand. Inorg Chem 48:4631–4633
21. Gao F, Cui L, Liu W, Hu L, Zhong Y-W, Li Y-Z, Zuo J-L (2013) Seven-coordinate lanthanide sandwich-type complexes with a tetrathiafulvalene-fused Schiff base ligand. Inorg Chem 52:11164–11172
22. Gao F, Zhang X-M, Cui L, Deng K, Zeng Q-D, Zuo J-L (2014) Tetrathiafulvalene-supported triple-decker phthalocyaninato dysprosium(III) complex: synthesis, properties and surface assembly. Sci Rep 4:srep05928
23. Ran Y-F, Steinmann M, Sigrist M, Liu S-X, Hauser J, Decurtins S (2012) Tetrathiafulvalene-based lanthanide coordination complexes: synthesis, crystal structure, optical and electrochemical characterization. Comptes Rendus Chim 15:838–844
24. Ueki S, Nogami T, Ishida T, Tamura M (2006) ET and TTF salts with lanthanide complex ions showing frequency-dependent ac magnetic susceptibility. Mol Cryst Liq Cryst 455:129–134
25. Pointillart F, le Guennic B, Cador O, Maury O, Ouahab L (2015) Lanthanide ion and tetrathiafulvalene-based ligand as a "magic" couple toward luminescence, single molecule magnets, and magnetostructural correlations. Acc Chem Res 48:2834–2842
26. D'Aleo A, Pointillart F, Ouahab L, Andraud C, Maury O (2012) Charge transfer excited states sensitization of lanthanide emitting from the visible to the near-infra-red. Coord Chem Rev 256:1604–1620
27. Pointillart F, Guennic BL, Golhen S, Cador O, Ouahab L (2013) Slow magnetic relaxation in radical cation tetrathiafulvalene-based lanthanide(III) dinuclear complexes. Chem Commun 49:11632–11634
28. Uzelmeier CE, Smucker BW, Reinheimer EW, Shatruk M, O'Neal AW, Fourmigué M, Dunbar KR (2006) A series of complexes of the phosphorus-based TTF ligand o-P2 with the metal ions Fe^{II}, Co^{II}, Ni^{II}, Pd^{II}, Pt^{II}, and Ag^{I}. Dalton Trans 5259–5268 AU4
29. Xiong J, Li G-N, Sun L, Li Y-Z, Zuo J-L, You X-Z (2011) Mono- and dinuclear Co/Ni complexes bearing redox-active tetrathiafulvaleneacetylacetonate ligands – syntheses, crystal structures, and properties. Eur J Inorg Chem 5173–5181
30. Guo YN, Xu GF, Gamez P, Zhao L, Lin SY, Deng R, Tang J, Zhang HJ (2010) Two-step relaxation in a linear tetranuclear dysprosium (III) aggregate showing single-molecule magnet behavior. J Am Chem Soc 132:8538–8539

31. Guo YN, Xu GF, Wernsdorfer W, Ungur L, Guo Y, Tang J, Zhang HJ, Chibotaru LF, Powell AK (2011) Strong axiality and Ising exchange interaction suppress zero-field tunneling of magnetization of an asymmetric Dy2 single-molecule magnet. J Am Chem Soc 133:11948–11951
32. Lin S-Y, Wernsdorfer W, Ungur L, Powell AK, Guo Y-N, Tang J, Zhao L, Chibotaru LF, Zhang H-J (2012) Coupling Dy3 triangles to maximize the toroidal moment. Angew Chem Int Ed 51:12767–12771
33. Guo Y-N, Ungur L, Granroth GE, Powell AK, Wu C, Nagler SE, Tang J, Chibotaru LF, Cui D (2014) An NCN-pincer ligand dysprosium single-ion magnet showing magnetic relaxation *via* the second excited state. Sci Rep 4:5471
34. Layfield RA (2014) Organometallic single-molecule magnets. Organometallics 33:1084–1099
35. Guo Y-N, Xu G-F, Guo Y, Tang J (2011) Relaxation dynamics of dysprosium(III) single molecule magnets. Dalton Trans 40:9953–9963
36. Zhang P, Zhang L, Tang J (2015) Lanthanide single molecule magnets: progress and perspective. Dalton Trans 44:3923–3929
37. Ungur L, Lin S-Y, Tang J, Chibotaru LF (2014) Single-molecule toroics in Ising-type lanthanide molecular clusters. Chem Soc Rev 43:6894–6905
38. Pointillart F, Cador O, Le Guennic B, Ouahab L (2017) Uncommon lanthanide ions in purely 4f single molecule magnets. Coord Chem Rev 346:150–175
39. Pointillart F, Le Gal Y, Golhen S, Cador O, Ouahab L (2011) Single-molecule magnet behaviour in a tetrathiafulvalene-based electroactive antiferromagnetically coupled dinuclear dysprosium(III) complex. Chem Eur J 17:10397–10404
40. Llunell M, casanova D, Cicera J, Bofill JM, Alemany P, Alvarez S (2013) SHAPE (version 2.1)
41. Rinehart JD, Long JR (2011) Exploiting single-ion anisotropy in the design of f-element single-molecule magnets. Chem Sci 2:2078–2085
42. Sievers J (1982) Asphericity of 4f-shells in their Hund's rule ground states. Z Für Phys B Condens Matter 45:289–296
43. Ungur L, Chibotaru LF (2011) Magnetic anisotropy in the excited states of low symmetry lanthanide complexes. Phys Chem Chem Phys 13:20086–20090
44. Ungur L, Chibotaru LF (2016) Strategies toward high-temperature lanthanide-based single-molecule magnets. Inorg Chem 55:10043–10056
45. Cosquer G, Pointillart F, Golhen S, Cador O, Ouahab L (2013) Slow magnetic relaxation in condensed versus dispersed dysprosium(III) mononuclear complexes. Chem Eur J 19:7895–7903
46. Jung J, Cador O, Bernot K, Pointillart F, Luzon J, Le Guennic B (2014) Influence of the supramolecular architecture on the magnetic properties of a DyIII single-molecule magnet: an ab initio investigation. Beilstein J Nanotechnol 5:2267–2274
47. da Cunha TT, Jung J, Boulon M-E et al (2013) Magnetic poles determinations and robustness of memory effect upon solubilization in a DyIII-based single ion magnet. J Am Chem Soc 135:16332–16335
48. Orbach R (1961) Spin-lattice relaxation in rare-earth salts. Proc R Soc Lond A 264:458–484
49. Pointillart F, Bernot K, Golhen S, Le Guennic B, Guizouarn T, Ouahab L, Cador O (2015) Magnetic memory in an isotopically enriched and magnetically isolated mononuclear dysprosium complex. Angew Chem Int Ed 54:1504–1507
50. Gatteschi D, Sessoli R (2003) Quantum tunneling of magnetization and related phenomena in molecular materials. Angew Chem Int Ed 42:268–297
51. Ishikawa N, Sugita M, Wernsdorfer W (2005) Nuclear spin driven quantum tunneling of magnetization in a new lanthanide single-molecule magnet: bis(phthalocyaninato)holmium anion. J Am Chem Soc 127:3650–3651
52. Ishikawa N, Sugita M, Wernsdorfer W (2005) Quantum tunneling of magnetization in lanthanide single-molecule magnets: bis(phthalocyaninato)terbium and bis(phthalocyaninato)dysprosium anions. Angew Chem Int Ed 44:2931–2935

53. Flores Gonzales J, Pointillart F, Ouahab L, Cador O. Hyperfine coupling and slow magnetic relaxation in isotopically enriched Dy(III) mononuclear single-molecule magnets. Submitted AU5
54. Ebenhöh W, Ehlers VJ, Ferch J (1967) Hyperfine-structure measurements on Dy^{161} and Dy^{163}. Z Für Phys 200:84–92
55. Childs WJ (1970) Hyperfine structure of $^5I_{8,7}$ atomic states of $Dy^{161,163}$ and the ground-state nuclear moments. Phys Rev A 2:1692–1701
56. Kishi Y, Pointillart F, Lefeuvre B, Riobé F, Guennic BL, Golhen S, Cador O, Maury O, Fujiwara H, Ouahab L (2017) Isotopically enriched polymorphs of dysprosium single molecule magnets. Chem Commun 53:3575–3578
57. Fujiwara H, Yokota S, Hayashi S, Takemoto S, Matsuzaka H (2010) Development of photofunctional materials using TTF derivatives containing a 1,3-benzothiazole ring. Phys B Condens Matter 405:S15–S18
58. Speed S, Feng M, Garcia GF et al (2017) Lanthanide complexes involving multichelating TTF-based ligands. Inorg Chem Front 4:604–617
59. Cole KS, Cole RH (1941) Dispersion and absorption in dielectrics I. Alternating current characteristics. J Chem Phys 9:341–351
60. Abragam A, Bleaney B (2012) Electron paramagnetic resonance of transition ions.Reprint edn. Oxford University Press, Oxford
61. Feng M, Pointillart F, Lefeuvre B, Dorcet V, Golhen S, Cador O, Ouahab L (2015) Multiple single-molecule magnet behaviors in dysprosium dinuclear complexes involving a multiple functionalized tetrathiafulvalene-based ligand. Inorg Chem 54:4021–4028
62. Jia C, Liu S-X, Tanner C, Leiggener C, Neels A, Sanguinet L, Levillain E, Leutwyler S, Hauser A, Decurtins S (2007) An experimental and computational study on intramolecular charge transfer: a tetrathiafulvalene-fused dipyridophenazine molecule. Chem Eur J 13:3804–3812
63. Pointillart F, Jung J, Berraud-Pache R et al (2015) Luminescence and single-molecule magnet behavior in lanthanide complexes involving a tetrathiafulvalene-fused dipyridophenazine ligand. Inorg Chem 54:5384–5397
64. Kuropatov V, Klementieva S, Fukin G, Mitin A, Ketkov S, Budnikova Y, Cherkasov V, Abakumov G (2010) Novel method for the synthesis of functionalized tetrathiafulvalenes, an acceptor–donor–acceptor molecule comprising of two o-quinone moieties linked by a TTF bridge. Tetrahedron 66:7605–7611
65. Pointillart F, Klementieva S, Kuropatov V, Gal YL, Golhen S, Cador O, Cherkasov V, Ouahab L (2012) A single molecule magnet behaviour in a D3h symmetry Dy(III) complex involving a quinone–tetrathiafulvalene–quinone bridge. Chem Commun 48:714–716
66. Soussi K, Jung J, Pointillart F, Guennic BL, Lefeuvre B, Golhen S, Cador O, Guyot Y, Maury O, Ouahab L (2015) Magnetic and photo-physical investigations into Dy(III) and Yb (III) complexes involving tetrathiafulvalene ligand. Inorg Chem Front 2:1105–1117
67. Huang G, Fernandez-Garcia G, Badiane I et al. Magnetic slow relaxation in a metal organic framework made of chains of ferromagnetically coupled single-molecule magnets. Chem Eur J. doi: https://doi.org/10.1002/chem.201800095
68. Zhang P, Jung J, Zhang L, Tang J, Le Guennic B (2016) Elucidating the magnetic anisotropy and relaxation dynamics of low-coordinate lanthanide compounds. Inorg Chem 55:1905–1911
69. Pointillart F, Guennic BL, Golhen S, Cador O, Maury O, Ouahab L (2013) A redox-active luminescent ytterbium based single molecule magnet. Chem Commun 49:615–617
70. Pointillart F, Golhen S, Cador O, Ouahab L Slow magnetic relaxation in a redox-active tetrathiafulvalene-based ferromagnetic dysprosium complex. Eur J Inorg Chem 2014, 2014:4558–4563
71. Pointillart F, Le Guennic B, Maury O, Golhen S, Cador O, Ouahab L (2013) Lanthanide dinuclear complexes involving tetrathiafulvalene-3-pyridine-N-oxide ligand: semiconductor radical salt, magnetic, and photophysical studies. Inorg Chem 52:1398–1408

72. Pointillart F, Guizouarn T, Lefeuvre B, Golhen S, Cador O, Ouahab L (2015) Rational design of a lanthanide-based complex featuring different single-molecule magnets. Chem Eur J 21:16929–16934
73. Belio Castro A, Jung J, Golhen S, Le Guennic B, Ouahab L, Cador O, Pointillart F (2016) Slow magnetic relaxation in unprecedented mono-dimensional coordination polymer of ytterbium involving tetrathiafulvalene-dicarboxylate linker. Magnetochemistry 2:26